

Theory of electrochemical monoatomic nanowires

E. P. M. Leiva, Cristián G. Sánchez, and P. Vélez

Unidad de Matematica y Fisica, Facultad de Ciencias Químicas, Universidad Nacional de Cordoba, 5000 Cordoba, Argentina

W. Schmickler

Department of Theoretical Chemistry, University of Ulm, D-89069 Ulm, Germany

(Received 18 January 2006; revised manuscript received 26 April 2006; published 19 July 2006)

Monoatomic nanowires in contact with an electrolyte can be charged by varying their potential with respect to a reference electrode. The principal properties of such wires have been explored within a model in which the wire is represented as jellium, and the electrolyte is treated on the Poisson-Boltzmann level. In addition, *ab initio* calculations have been performed for the structure of monoatomic gold and silver wires. Due to the cylindrical geometry the interfacial capacity is much larger than for a planar geometry, and mass transport is enhanced. The work function is higher than for bulk electrodes, which entails a shift of the point of zero charge to high potentials. This should make it possible to reach very high negative charge densities on electrochemical nanowires. As a consequence, such wires may have different catalytic properties than bulk electrodes.

DOI: [10.1103/PhysRevB.74.035422](https://doi.org/10.1103/PhysRevB.74.035422)

PACS number(s): 68.65.La, 82.45.Aa

I. INTRODUCTION

During the last decade, monoatomic metal wires have been the subject of a vast amount of research. They exhibit interesting mechanical, electrical and magnetic properties, which have been investigated both theoretically and experimentally; recent work has been reviewed in Refs. 1 and 2 where an extended list of references can be found.

The large majority of these investigations has been performed in vacuum or air. Only little work has been done on monoatomic wires in contact with an electrolyte solution. This is a pity, because in an electrochemical environment the potential of the wire can be controlled, so there is an extra electrical variable. As a consequence, the wire can be charged, the countercharge residing in the solution. As we shall demonstrate in this work, the resulting charge densities can be much higher than on flat electrodes, making it possible to study electrochemical processes in the presence of very high fields.

Much of the pioneering experimental work on electrochemical monoatomic wires has been performed by the group of Tao and co-workers. In particular, this group has devised convenient ways for the fabrication of such wires with the aid of devices based on the scanning tunneling microscope.^{3,4} If the metal, of which the wire is composed, is soluble in the electrolyte solution, the thickness of the wire can be controlled by stepping the potential into a region in which deposition or dissolution of the wire occurs. If the metal is insoluble the potential can be used to charge the wire or to adsorb certain species from the solution.^{5,6} Such changes have been found to have a pronounced effect on the properties of the wires, in particular on their conductivity.

Thus, charged nanowires are a fascinating area of research. But though there has been intensive theoretical research on nanowires in general, the consequences of changing the potential and the charge of such wires within an electrochemical environment have not been explored. Here we embark on such an investigation.

Since this, to the best of our knowledge, is the first systematic theoretical exploration of electrochemical nanowires,

we will approach the topic from several directions, and consider both the wire itself and the adjacent solution. Basic properties of charged nanowires will be explored within the jellium model, and the specific properties of gold and silver wires will be calculated by *ab initio* methods. The distribution of the ions in the solution and its effect on the capacity will be determined from the Poisson-Boltzmann equation. Due to the cylindrical geometry, the capacity is greatly enhanced, and so is diffusion towards or away from the nanowire. We will conclude our investigations by some comments on the energetics of the interface, and finally we discuss the consequences of our findings for reactions and processes at nanowires.

II. CHARGED JELLIUM WIRES

To a large extent, our understanding of the metal side of electrochemical interfaces is based on the jellium model.^{7,8} It describes the response of the electronic density to the double layer field, explains why the interfacial capacity depends on the nature of the metal, and predicts the correct order of magnitude for the capacity of *sp* metals.⁹ So it is natural to use the same model as a starting point to explore charged nanowires.

Thus, we model the monoatomic wire as an infinite cylindrical jellium wire (see Fig. 1). It is a well-known deficiency of jellium that its surface energy becomes negative for high electronic densities; therefore we have performed our calculations for a low density with a Wigner-Seitz radius of $r_s=3$ a.u., so that the surface has a positive energy of the same order of magnitude as is found in low density metals. The radius R_w of the corresponding monoatomic wire, which we identify with the radius of the constant positive background charge, is not known *a priori*. If the jellium corresponded to a monovalent metal with fcc or bcc structure, the radius of a monoatomic wire, with an interatomic distance equal to the shortest distance in the lattice, would be about $R_w=2.6$ a.u., and the calculations that we show here have been performed for this thickness.

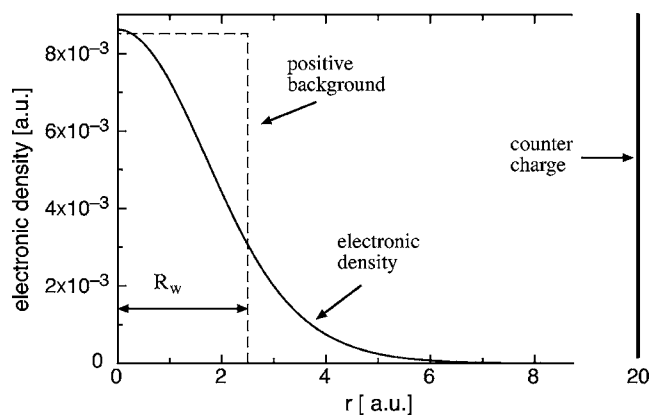


FIG. 1. A charged jellium nanowire.

Because of the cylindrical symmetry, the electronic wave functions for the wire take the form

$$\psi(r, \phi, z) = \chi(r)\exp(in\phi)\exp(ikz), \quad n \in \mathbb{Z}. \quad (1)$$

For the given dimensions, there is only one solution for the radial wave function $\chi(r)$ with an energy below the Fermi level, and only states with angular momentum quantum number $n=0$ contribute. States with wave numbers k ranging from zero to an upper level k_F are occupied, where k_F must be chosen such that the wire is uncharged or carries a specific charge. The radial wavefunction was obtained self-consistently through an iterative procedure starting from an approximate solution. There are no oscillations in the density, because there is only one radial wavefunction. Similar calculations for jellium wires have been carried out by several groups (e.g., Ref. 10); the new feature in our work is the charging of the wire.

The wire can be charged by making the total electronic charge per length of the wire greater or lower than the positive background charge. Meaningful calculations can only be performed for a system that is electrically neutral. The countercharge required for electroneutrality was placed on a concentric cylinder with a radius $R_{\text{out}}=20$ a.u., sufficiently large that the electronic density vanishes there (see Fig. 1). The total energy of the system depends on the position of this counter charge because of the classical electrostatic energy stored in the space between the wire and the counter charge. However, we are not interested in this electrostatic energy, because in a real electrochemical system the space surrounding the wire is filled with a solution, whose properties we will consider below. Therefore, for a given excess charge, we have calculated the classical electrostatic energy stored in the region between the radii R_w of the wire and R_{out} of the countercharge, and subtracted this energy from the total energy of the system.

It is one of the conceptual advantages of jellium that its surface is well defined by the edge of the positive background charge—in contrast, in a real metal there is some arbitrariness in the choice of the surface. This makes it possible to calculate the surface energy f_s of the jellium wire—as discussed above, without the classical electrostatic part outside the wire—as a function of the surface charge

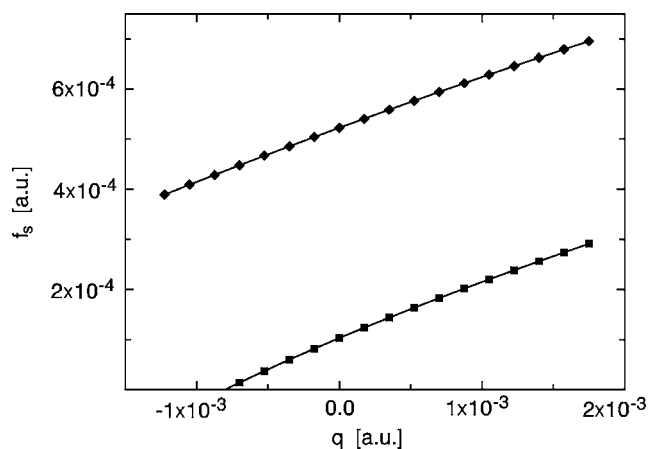


FIG. 2. Surface energy per unit area of a monoatomic jellium wire as a function of the surface charge density q ; the classical electrostatic energy outside the wire has been subtracted. Upper curve (\blacklozenge) $R_w=2.6$ a.u., bottom curve (\blacksquare) flat semi-infinite jellium.

density q , and compare it with the surface energy of flat, semi-infinite jellium; Fig. 2 shows the results. As may be expected, the surface energy of the wire is substantially higher than that of flat jellium. The slope of the f_s vs q curve gives the energy required to take an electron out of the jellium; this is the electrochemical potential $\tilde{\mu}$ of the electrons, and it is therefore always positive. In particular, the slope at $q=0$ gives the work function Φ . Of course, the work function can also be directly obtained from the electronic density for the uncharged systems, and the equality of the two values for the work function obtained by these different procedures is a useful check on the accuracy of the calculations. The work functions of our monoatomic wire is lower than the value for flat jellium: $\Phi=2.84$ eV compared with $\Phi=3.47$ eV for flat jellium. This lowering of the work function is caused by the zero-point energy that the radial part of the wave function acquires due to the radial constraint. We shall see later, that this is a specialty of jellium that is not found in gold and silver wires.

Of particular interest is the response of the electronic density to an electric field, or to the presence of an excess charge. Figure 3 shows the distribution of small excess charges; just as in planar jellium,¹¹ a large part resides in front of the surface. A negative charge extends somewhat further beyond the surface than a positive excess does, because it can simply be created by extending the electronic tail further into the vacuum (or the solution), while outside the jellium edge a positive excess charge can only be formed by a retraction of the electronic tail.

This distribution of the excess charge affects the capacity of the interface. As was shown by Lang and Kohn,¹¹ at planar surfaces, due to the spill-over of the electrons, the effective position of the image plane lies a certain distance x_{im} in front of the jellium edge. This is also the effective position of the plate of a capacitor. On planar jellium, this distance is of the order of 1–2 a.u., and is thus entirely negligible for normal, macroscopic capacitors. However, the electric double layer at the interface between a metal and a concentrated electrolyte solution can be viewed as a capacitor with an

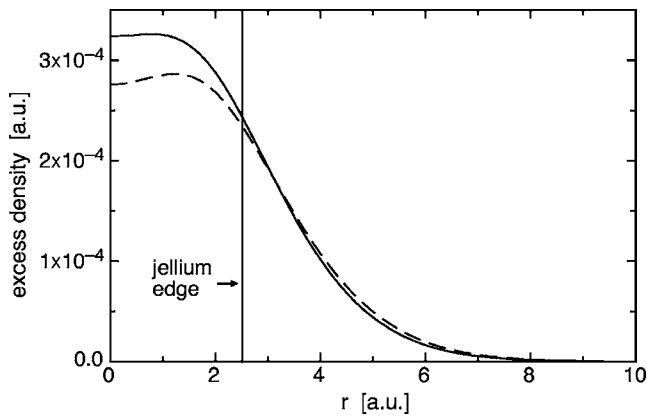


FIG. 3. Distribution of a small surface charge density at a nanowire of radius $R_w=2.5$ a.u. Full line: $q=3.5 \times 10^{-4}$ a.u., dashed line: $q=-3.5 \times 10^{-4}$ a.u.

effective plate separation of a few Å, and therefore even a small effective shift of the metal surface is quite significant.

The concept of an image plane has to be modified for cylindrical geometry. For this purpose we consider a classical cylindrical condenser with inner and outer radii R_{in} and R_{out} ; its inverse capacity per unit length is given by

$$1/C = 2 \ln \frac{R_{out}}{R_{in}}. \quad (2)$$

For a parallel plate capacitor, the inverse capacity is proportional to the plate separation, and for a jellium plate this is diminished by x_{im} . For a jellium nanowire it is therefore natural to define the shift d_{im} of the effective radius through the relation

$$1/C_j = 2 \ln \frac{R_{out}}{R_w + d_{im}}, \quad (3)$$

where C_j is the capacity per length in our system consisting of the jellium wire and the concentric counter charge. This definition is independent of R_{out} as long as it is sufficiently large, i.e., if it does not affect the electronic tail, since R_{out} cancels in the difference $1/C_j - 1/C$. In atomic units, the capacity per unit length is dimensionless.

As is evident from Fig. 3, the electronic response of the wire is nonlinear even at moderate charge densities, therefore the capacity is a function of the surface charge density. This is generally observed in electrochemical systems; the quantity that is usually measured is the differential capacity at a given potential or surface charge, which is easily obtained from impedance spectroscopy. Therefore we understand the capacity of Eq. (3) as the differential capacity $C_j = dq_l / \Delta V$, where q_l is the charge per unit length, and ΔV the potential drop between the two plates. In this way d_{im} is defined as a differential quantity as well. Of course, for a linear capacitor the differential capacity equals the normal capacity $q_l / \Delta V$. Henceforth we shall consider differential capacitances only.

The variation of the shift d_{im} with the surface charge density can be seen in Fig. 4. It is higher at negative charge densities, because the electrons extend further beyond the jellium edge. For comparison we note that at a planar, un-

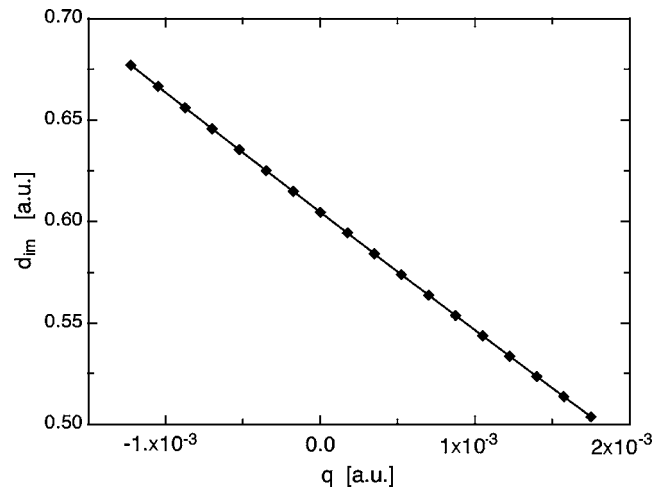


FIG. 4. Effective shift d_{im} of the nanowire radius as a function of the surface charge density.

charged jellium surface of the same density the effective shift of the image plane is about 1.3 a.u. and thus a little higher.

III. *ab initio* CALCULATIONS FOR GOLD AND SILVER

Jellium is a good model to explore basic electronic effects, but it cannot provide quantitative results for *sd* or transition metals, which are commonly employed as materials for electrochemical nanowires. We have therefore performed *ab initio* calculations for the structure of monowires composed of the metals gold and silver, using the SIESTA^{12,13} package; both these metals are popular electrode materials, and monoatomic gold wires have in fact been studied experimentally in electrochemical environments.⁴

Of particular interest is the equilibrium distance between the atoms, and its possible variation with the charge. This poses a principle problem, because, just as with jellium, meaningful calculations can only be performed for neutral systems, with the counter charge placed concentrically at a certain distance from the wire. Therefore, the total energy, which has to be minimized in order to determine the equilibrium distance, always contains the energy of the electric field between the wire and the counter charge. In a real electrochemical system the counter charge resides on the ionic space charge, which will be considered in the next section, and the total system energy would include the energy stored in this space-charge region. Fortunately, the variation of the energy of the wire with the interatomic distance is solely determined by the properties of the wire itself; the energy of the electric field outside plays no role, as long as the countercharge is placed at a reasonable distance, i.e., less than about 20 Å. For this reason it is also not important, if this energy minimization with respect to the distance is made at constant charge or at constant potential, a point that we will discuss further below.

For both metals the equilibrium distance in the wire is significantly lower than in the bulk system (see Fig. 5), where it is about 2.89 Å for both metals. Such a decrease of the binding length in wires has been observed before.¹⁴ The

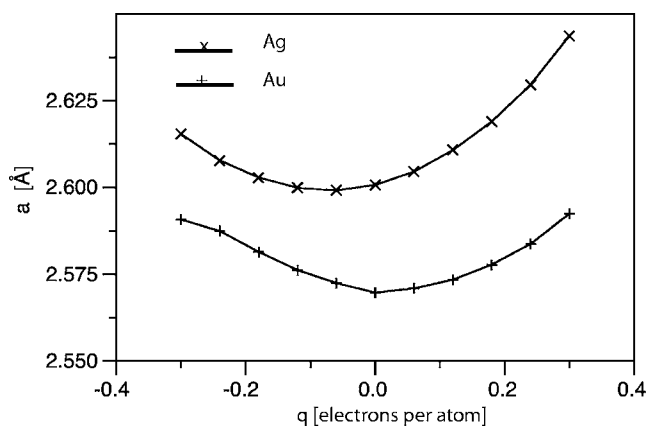


FIG. 5. Interatomic distance as a function of the excess charge per atom. The upper curve is for silver, the lower for gold.

interatomic separation attains its minimum near zero charge; due to Coulomb repulsion, it increases with the absolute value of the charge.

There is a considerable change in the work functions of the wires compared with the values for semi-infinite crystals. We obtained $\Phi=6.79$ eV for the gold wire and $\Phi=5.41$ eV for silver. For comparison: the value for Au(111) is $\Phi=5.31$ eV and for Ag(111) $\Phi=4.74$ eV. This has significant consequences for electrochemical experiments: the potential, at which an electrode is uncharged (point of zero charge) differs from the work function only by an additive constant.¹⁵ Therefore, it will be shifted by a large amount towards higher values.

IV. SPACE-CHARGE CAPACITY OF THE SOLUTION

In this section we consider a classical, perfectly conducting cylindrical wire of radius R in contact with an electrolyte solution. An excess charge on the wire attracts ions of opposite sign from the solution, and repels ions of the same sign. This results in a space-charge region surrounding the wire, whose total excess charge balances that of the wire. In a simple model the ions can be regarded as point charges, and the solvent as a dielectric continuum with a dielectric constant ϵ . The distribution of the particles is then governed by a combination of Poisson's equation with the Boltzmann distribution. This model is known as the Gouy-Chapman theory in electrochemistry, as the Debye-Huckel theory in the physical chemistry of solutions, and in semiconductor physics the same model is used to calculate the extension of space-charge regions and the resulting capacity.

In order to be specific, we consider the case where the solution contains two types of ions, cations and anions with charge numbers $\pm z$. Because of the cylindrical symmetry, the electric potential $\phi(r)$ is a function of the radial distance r from the center of the wire; we set $\phi(\infty)=0$. The decay of the potential is governed by the inverse Debye length: $\kappa=[(2z^2e_0^2n_0)/(\epsilon\epsilon_0k_B T)]^{1/2}$, where n_0 is the concentration of the ions in the bulk of the solution, and the other symbols have their usual meaning. It is convenient to introduce a dimensionless potential and radius through

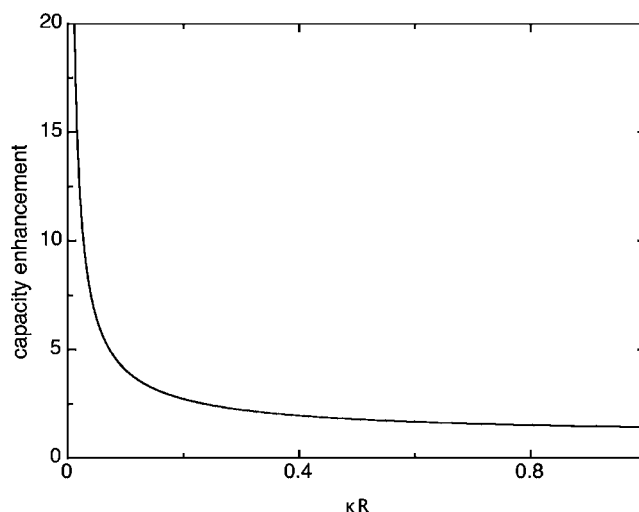


FIG. 6. Enhancement of the capacity per unit area compared with planar geometry for the linear Poisson-Boltzmann equation.

$$g(\rho) = \frac{ze_0}{k_B T} \phi(\rho), \quad \rho = \kappa r. \quad (4)$$

The Poisson-Boltzmann equation then takes on the simple form

$$\frac{d^2g}{d\rho^2} + \frac{1}{\rho} \frac{dg}{d\rho} = \sinh g. \quad (5)$$

For small excess charges $\sinh g$ can be expanded to first order. The resulting linear Poisson-Boltzmann equation is of the Bessel type and easily solved. The normalized potential is proportional to the Bessel function $K_0(\rho)$. The capacity of the wire per unit area is given by

$$C_w = \epsilon\epsilon_0\kappa \frac{K_1(\kappa R)}{K_0(\kappa R)}, \quad (6)$$

where R is the radius of the wire. $\epsilon\epsilon_0\kappa$ is just the capacity for a planar electrode, so the ratio of the two Bessel functions gives the enhancement for a cylindrical symmetry. This enhancement factor can reach quite significant values, particularly for thin wires and small inverse Debye lengths, i.e., for low ionic concentrations (see Fig. 6). To give some idea about the magnitudes involved: For a 10^{-1} M solution of a univalent aqueous electrolyte $\kappa \approx 10^{-1} \text{ \AA}^{-1}$, for a 10^{-3} M solution $\kappa \approx 0.01 \text{ \AA}^{-1}$. The effective radius of the wire should probably be taken about 3 \AA larger than the physical radius, since it is usually assumed that the ions are separated from the electrode by their solvation shells, which comprises one layer of water. So under normal experimental conditions we may expect enhancements of the order of 1.5 to 10.

The nonlinear version of Eq. (5) is easily integrated numerically; Fig. 7 shows some results calculated for $R=5 \text{ \AA}$. As with planar electrodes, the capacity has its minimum at zero charge. The large enhancement is also evident in the nonlinear case, and it does not vary much with the charge density.

The capacity calculated here has been for a perfect metal conductor. In a real wire this capacity will be enhanced by

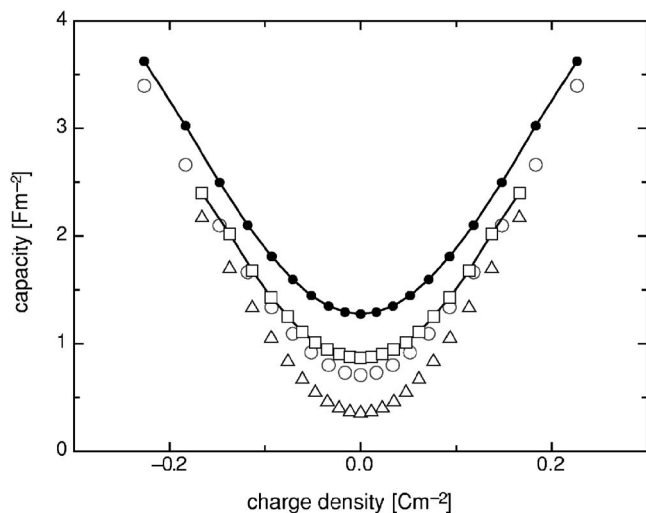


FIG. 7. Differential interfacial capacity per unit area of a cylindrical wire with radius $R=5 \text{ \AA}$. \bullet : $\kappa=0.1 \text{ \AA}^{-1}$; \square : $\kappa=0.05 \text{ \AA}^{-1}$; \circ : planar electrode with $\kappa=0.1 \text{ \AA}^{-1}$, \triangle : planar electrode with $\kappa=0.05 \text{ \AA}^{-1}$.

the shift of the effective surface d_{im} derived above within the jellium model.

V. LINE TENSION

Electrodes are surfaces of constant potential, and not of constant charge. Therefore the correct thermodynamic potential is not the surface free energy but the surface tension γ .^{9,16} The latter is obtained from the free energy per unit area f_s through a Legendre transformation

$$\gamma = f_s - q \partial f_s / \partial q = f_s + \frac{q}{e_0} \tilde{\mu} = f_s - q \phi, \quad (7)$$

where $\tilde{\mu} = -e_0 \phi$ is the electrochemical potential of the metal electrons, and ϕ is the electrode potential on the absolute scale; the latter differs from the conventional hydrogen scale by a constant, which is of the order of $4.5 \pm 0.2 \text{ V}$ (see Ref. 9). For a real wire, the surface area is not well defined, but the energy per unit length is. Therefore it is more natural to consider the corresponding quantities per unit length. So we use the line tension γ_l , which is obtained from the free energy f_l per unit length by the corresponding transformation

$$\gamma_l = f_l - q_l \partial f_l / \partial q_l = f_l - q_l \phi, \quad (8)$$

where q_l is the charge per unit length. γ_l is analogous to the surface tension. The following relations hold:

$$\partial \gamma_l / \partial \phi = -q_l, \quad \partial^2 \gamma_l / \partial \phi^2 = -C, \quad (9)$$

where C is the capacity per unit length. These relations follow directly from the transformation in Eq. (8), and are the one-dimensional analogs to the well-known relations for the surface tension.⁹

The free energies in Eqs. (7) and (8) consist of the corresponding energy of the wire and the free energy stored in the space-charge region in the solution. In order to obtain some idea about the line tension of nanowires we performed model

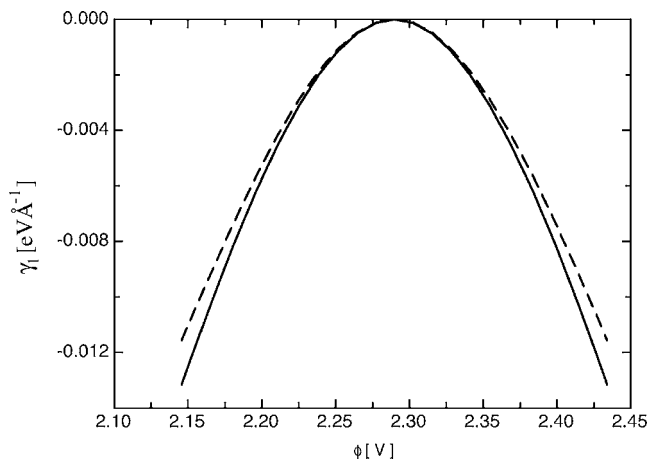


FIG. 8. Examples of the line tension for a gold monoatomic wire as a function of the electrode potential; the latter is given on the standard hydrogen scale (SHE) using a value of 4.5 V for the vacuum scale (Ref. 9). Full line: $\kappa=0.1 \text{ \AA}$, dashed line: $\kappa=0.01 \text{ \AA}$. The value at the maximum (pzc) has been set to zero.

calculations for a gold wire, proceeding in the following way: The *ab initio* calculations give the total electronic energy of the wire including the electrostatic energy stored outside. From this we subtracted the classical energy stored in the field outside the wire, assuming that the radius of the wire equals the crystallographic radius of a gold atom (1.44 \AA), and added the free energy stored in the ionic space-charge region. In this way we obtained the free energy per length f_l as a function of the charge q_l , and from the transformation (8) the line tension. Figure 8 shows some examples of the calculated dependence of the line tension of a gold wire in contact with a solution as a function of the electrode potential. Since the absolute value of the line tension of a solid wire cannot be measured, we have set the value at the point of zero charge equal to zero. The line tension shows the behavior familiar from the surface tension: It attains its maximum at the pzc, and has roughly the form of an inverted parabola. The main difference to normal electrocapillary curves is the shift of the pzc to highly positive values, and the greater curvature, which is caused by the higher capacity. The curve calculated for an inverse Debye length of $\kappa=0.01 \text{ \AA}$ shows a smaller curvature because the capacity is less, as discussed above.

VI. DIFFUSION AT A NANOWIRE

Diffusion towards small objects is greatly enhanced compared to planar diffusion. In electrochemistry, this fact is exploited in the technique of microelectrodes, which, as the name suggests, operates on the micrometer scale. At monoatomic nanowires this enhancement is extreme.

In order to obtain a quantitative estimate for the diffusion current, we consider the idealized case of a cylinder of radius R embedded in an infinite electrolyte. The time-dependent diffusion equation

$$\frac{\partial c}{\partial t} = -D \Delta c \quad (10)$$

for a species with concentration c and diffusion coefficient D is readily solved in cylindrical coordinates. To be specific,

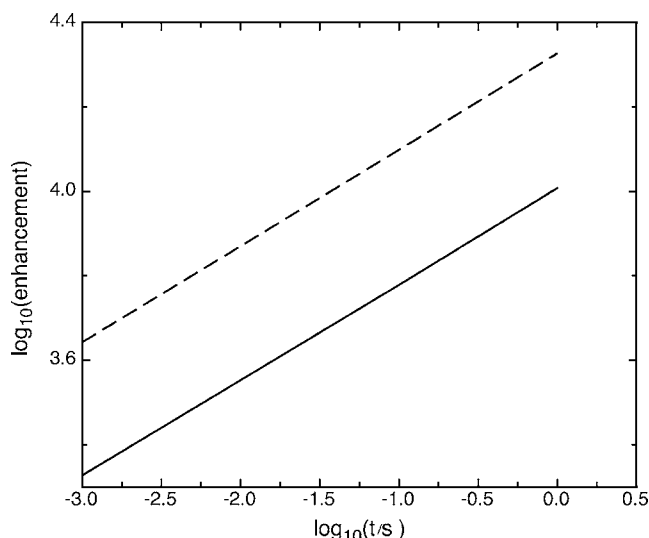


FIG. 9. Enhancement of the diffusion current towards a cylindrical wire of radius 1.5 Å. Full line: $D=10^{-6}$ cm² s⁻¹, dashed line: $D=5 \times 10^{-6}$ cm² s⁻¹.

we consider the case in which the species at first has a constant concentration in the solution, i.e., $c(r,t)=c_0$ for $t \leq 0$. At the time $t=0$ the electrode potential is stepped to a value such that every molecule at the surface is immediately consumed, i.e., $c(R,t)=0$ for $t > 0$. The resulting concentration profile $c(r,t)$ is given in the book by Crank.¹⁷ The quantity of interest to us is the current density towards the electrode

$$j = -D \left. \frac{\partial c(r,t)}{\partial r} \right|_{r=a}. \quad (11)$$

Using the results from Ref. 17 we obtain

$$\left. \frac{\partial c(r,t)}{\partial r} \right|_{r=R} = -\frac{2}{\pi\sqrt{Dt}} \int_0^\infty \times e^{-x^2} \frac{J_1(x\tilde{R})Y_0(x\tilde{R}) - Y_1(x\tilde{R})J_0(x\tilde{R})}{J_0^2(x\tilde{R}) + Y_0^2(x\tilde{R})} dx, \quad (12)$$

where $\tilde{R}=R/\sqrt{Dt}$ is the ratio of the radius of the wire to the diffusion length; the J and Y symbols denote the indicated Bessel functions. At a planar electrode, the corresponding gradient is

$$\left. \frac{\partial c(x,t)}{\partial x} \right|_{x=0} = -(\pi Dt)^{-1/2}. \quad (13)$$

The ratio of the gradients given by Eqs. (12) and (13) defines the enhancement factor for transport to a nanowire. It is of the order $1/\tilde{R}$, i.e., the ratio of the diffusion length to the radius of the wire, and it therefore increases with time. Figure 9 shows some representative values for the time scale of

10^{-3} to 1 s that is typically covered in electrochemical experiments. Enhancements of the order of 10^3 – 10^4 may be expected over this range.

VII. DISCUSSION

From a practical point of view, our most important findings are the large capacities of the wires, which makes it possible to achieve very high fields, and the large rise of the work function for gold and silver wires, which entails a concomitant shift of the potential of zero charge. This has far-reaching consequences for the electrochemistry of such wires. For example, on gold electrodes, the so-called double-layer region, in which the electrode can be examined without interference from oxygen or hydrogen evolution, is roughly between -0.4 to 0.8 V vs SHE (standard hydrogen electrode). On bulk gold electrodes, the potential of zero charge lies somewhere in the middle of this region, its exact value depending on the crystal face. According to our calculations, this is now shifted by more than one volt towards more positive potentials. This implies, that in the whole accessible region a gold monoatomic wire will be negatively charged, the charge increasing dramatically towards negative potentials.

According to classical thermodynamic considerations, electrochemical processes are governed by the electrode potential only. However, in recent years it has transpired, that the electric field plays a dominant role in many processes. Examples include not only the obvious case of ionic adsorption, but also surface processes such as step bunching,^{18,19} surface reconstruction,²⁰ and adatom diffusion.²¹ In addition, it has been suggested that the hydrogen evolution reaction is enhanced by a negative field, which turns the hydronium ion into a favorable orientation with its protons directed towards the metal.²² Nanowires offer the possibility, to investigate such processes at ordinary potentials and very high negative fields directed towards the wire.

As we pointed out in the introduction, so far only few experiments have been performed on nanowires in ionic solutions, so we cannot relate our results to experimental data. However, we would like to suggest that the control of the thickness of nanowires by metal deposition and dissolution, as performed in the work of Tao *et al.*,^{5,6} only works because of the special conditions encountered at the wires. Usually, the spatial constraints in the region between an STM tip and an electrode surface makes it very difficult to control metal deposition and dissolution. However, the high fields at the wire, combined with the rapid transport, favor reactions at the wire over reactions at the neighboring flat surfaces. Finally, we suggest that the unusual, potential dependent conductivities observed at gold nanowires may also be related to the extremely high fields.

ACKNOWLEDGMENT

Financial support by the Deutsche Forschungsgemeinschaft is gratefully acknowledged.

- ¹N. Agrait, A. L. Yeyati, and J. M. van Ruitenbeek, *Phys. Rep.* **377**, 81 (2003).
- ²D. R. Bowler, *J. Phys.: Condens. Matter* **16**, R721 (2004).
- ³C. Z. Li, A. Bogozzi, W. Huang, and J. J. Tao, *Nanotechnology* **10**, 221 (1999).
- ⁴H. X. He, S. Boussaad, B. Q. Xu, C. Z. Li, and N. J. Tao, *J. Electroanal. Chem.* **522**, 167 (2002).
- ⁵C. Shu, C. Z. Li, H. X. He, A. Bogozim, J. S. Bunch, and N. J. Tao, *Phys. Rev. Lett.* **84**, 5196 (2000).
- ⁶N. J. Tao, C. Z. Li, and H. X. He, *J. Electroanal. Chem.* **492**, 81 (2000); A. Bogozzi, O. Lam, H. X. He, C. Z. Li, N. J. Tao, L. A. Nagahara, I. Amlani, and R. Tsu, *J. Am. Chem. Soc.* **123**, 4585 (2001).
- ⁷W. Schmickler and D. Henderson, *Prog. Surf. Sci.* **22**, 323, (1986).
- ⁸S. Amokrane and J. P. Badiali, *Modern Aspects of Electrochemistry* (Plenum Press, New York, 1986), Vol. 22.
- ⁹W. Schmickler, *Interfacial Electrochemistry* (Oxford University Press, New York, 1996).
- ¹⁰There are numerous papers dealing with the properties of uncharged wires, e.g., C. Yannouleas, E. N. Bogachek, and U. Landman, *Phys. Rev. B* **57**, 4872 (1998); J. Frantti, V. Lantto, S. Nishio, and M. Kakihana, *ibid.* **59**, 12652 (1999).
- ¹¹N. D. Lang and W. Kohn, *Phys. Rev. B* **3**, 1215 (1971).
- ¹²The Siesta method for *ab initio* order-*N* materials simulation Jos M. Soler, Emilio Artacho, Julian D. Gale, Alberto Garca, Javier Junquera, Pablo Ordejn, and Daniel Snchez-Portal, *J. Phys.: Condens. Matter* **14**, 2745 (2002).
- ¹³The method for the study of charged one dimensional systems was developed and implemented in SIESTA by C. G. Sánchez, J. J. Kohanoff, and E. P. M. Leiva.
- ¹⁴J. A. Torres, E. Tosatti, A. Dal Corso, F. Ercolessi, J. J. Kohanoff, F. D. Di Tolla, and J. M. Soler, *Surf. Sci.* **426**, L441 (1999).
- ¹⁵S. Trasatti, in *Advances in Electrochemistry and Electrochemical Engineering*, edited by H. Gerischer and C. W. Tobias (1977), Vol. 10, pp. 213–321.
- ¹⁶W. Schmickler and E. Leiva, *J. Electroanal. Chem.* **453**, 61 (1998).
- ¹⁷J. Crank, *The Mathematics of Diffusion* (Oxford University Press, Oxford, 1979).
- ¹⁸H. Ibach and W. Schmickler, *Phys. Rev. Lett.* **91**, 016106 (2003).
- ¹⁹M. Giesen, H. Ibach, and W. Schmickler, *Surf. Sci.* **573**, 24 (2004).
- ²⁰E. Santos and W. Schmickler, *Chem. Phys. Lett.* **400**, 26 (2005).
- ²¹Margret Giesen, Guillermo Beltramo, Sabine Dieluweit, Jorge Müller, Harald Ibach, and W. Schmickler, *Surf. Sci.* **595**, 127 (2005).
- ²²O. Pecina and W. Schmickler, *Chem. Phys.* **228**, 265 (1998).